INFLAMMATORY AND MORPHOLOGICAL CHARACTERIZATION OF A FOREIGN BODY RETINAL RESPONSE

M. DI PAOLO[1], D. GHEZZI[2], M.R. ANTOGNAZZA[3], M. METE[4], G. FREDDI[5], I. DONELLI[5], R. MACCARONE[1], G. PERTILE[4], G. LANZANI[3], F. BENFENATI[2] and S. BISTI[1]

[1]Department of Biotechnology and Applied Clinical Science, University of L'Aquila, Italy; [2]Department of Neuroscience and Brain Technologies, Istituto Italiano di Tecnologia, Genoa, Italy; [3]Center for Nano Science and Technology, Istituto Italiano di Tecnologia, Milan, Italy; [4]Ohpthalmology Operative Unit, Ospedale Sacro Cuore - Don Calabria, Negrar, Italy; [5]Innovhub-SSI, Silk Division, Milan, Italy

Substitutive strategies are promising approaches to apply when retinal diseases lead to total blindness. The first test to be performed is an *in-vivo* biocompatibility study. We evaluated tissue reactions following sub-retinal implantation of a foreign body. Experiments were performed on Royal College of Surgeons non-dystrophic congenic rats (RCS-rdy). Two-three-month-old animals were implanted with a piece of silk and left them to recover for at least 3 weeks before starting the experimental protocol. Immunofluorescence assays were performed in both implanted and non-implanted rats to verify the correct position of the prosthesis and its long-term tolerability. The expression of inflammatory markers was monitored on retinas (GFAP) after implantation. Results suggest a good tolerability of the foreign body. Morphological analysis of implanted eye confirmed that the silk did not seriously alter the structure of the healthy retina. Immuno-inflammation markers indicated a modest inflammatory reaction and suggested long-term tolerability. In conclusion, our results confirm the viability of silk as support of sub-retinal prosthesis as silk does not induce adverse reactions.

Retinal degenerative diseases, such as age-related macular degeneration (AMD) and *Retinitis pigmentosa* (RP), are the leading cause of photoreceptor lost and blindness in adults (Coleman et al. 2008; Curcio et al. 1996; Liu et al. 2015). Restoration of visual perception is one of the new frontiers for prosthetic devices that have great potentiality in coping with these devastating disorders. The preferential targets for implanting sub-retinal visual prostheses are diseases affecting retinal pigment epithelium and photoreceptors but preserving, at least partially, inner retinal layers (Light et al. 2014; Maghami et al. 2014). These devices have to be associated with a physical support as biocompatible as possible to maintain correct function and position. We evaluated the amount of retinal reaction against a possible biological scaffold for retinal prostheses, silk fibroin.

MATERIALS AND METHODS

Preparation of silk

Bombyx mori cocoons were supplied by CRA, Council of Research and Experiments in Agriculture, Apiculture and Sericulture Unit, Padua, Italy. Lithium bromide (LiBr) extra pure was obtained from Merck. Dialysis tubing

Key words: retina, silk, biocompatibility, visual prosthesis

Corresponding author:
M. Di Paolo,
Via Tiburtina Valeria n° 102,
65128, Pescara, Italy
Tel.: +39 3206729342; +44 7732580154
e-mail: mattiadipaolo@gmail.com

2279-5855 (2015)

cellulose membrane (MW cut-off = 12,000 Da) were obtained from Sigma Aldrich. Cocoons were degummed in autoclave at 120°C for 15' and then rinsed with distilled water to remove sericin. After room temperature drying and storage under controlled conditions (T = 20±2°C and relative humidity = 65±2%), SF fibres were dissolved in a 9.3M LiBr aqueous solution (T = 60±2°C, t = 3 h) to obtain a 10% w/v SF solution. The solution was then diluted with distilled water to obtain a 2% w/v SF solution and dialyzed against distilled water for 3 days using dialysis tubing cellulose membrane to remove LiBr salt. SF films were prepared by pouring 22.5 ml of SF solution into Teflon Petri Dishes (ø = 75 mm), followed by casting under fume hood at room temperature until complete solvent evaporation and thermal drying at 105°C for 20 h.

Animal care and surgical procedures

Royal College of Surgery non-dystrophic congenic animals (RCS-rdy/LAV) (UCSF School of Medicine San Francisco, California) were housed in standard conditions with *ad libitum* access to food and water under a 12/12-hour light/dark cycle. All animal manipulations and procedures were performed in accordance with the guidelines established by the European Community Council (Directive 2012/63/EU of 22 September 2010) and were approved by the Italian Ministry of Health.

Animals were implanted at mean age of 85 days in the right eye and the experimental protocol started two weeks after surgery. Ketamine/xylazine anaesthesia was used with intra peritoneal injection of 100 mg/kg ketamine, 12 mg/kg xylazine (Ketavet 100 mg/ml, Intervet production srl; Xylazine 1 g, Sigma Co.). Sub-retinal implantation technique was previously described by other groups (Butterwick et al. 2009). Briefly, a 1.5 mm incision was made through the sclera and choroid, 1.5 mm posterior to the limbus and the implant was placed into the sub-retinal space using a custom-made implantation tool. The sclera and conjunctiva were electrocautery sutured.

Five animals were used in each group. Implanted eyes were compared with the fellow eye (internal control group) and healthy control group.

Preparation of explanted retinas

The superior aspect of the eye was marked with an indelible marker by a stitch in the conjunctiva, after euthanasia with CO2. Thereafter, the eyes were dissected free and fixed by immersion in 4% paraformaldehyde fixative buffer at 4°C for 1 h. After three rinses in 0.1 M phosphate-buffered saline (PBS), eyes were left overnight in a 15% sucrose solution to provide cryoprotection. Eyes were embedded in mounting medium (Tissue Tek OCT compound; Sakura Finetek, Torrance, CA) by snap freezing in liquid nitrogen. Cryosections were cut at 20 µm (CM1850 Cryostat; Leica, Wetzlar, Germany) with the eyes oriented so that the sections extended from superior to inferior edge. Sections were mounted on gelatin and poly-L-lysine-coated slides and were then dried overnight in 50°C oven and stored at −20°C until processed.

Immunohistochemistry: Iba1 and GFAP staining

Retinal sections were washed with 0.1 M PBS (twice for 10 min) and incubated in 10% normal goat serum in 0.1 M PBS for 1 h at room temperature, to block non-specific binding. Sections were then incubated overnight at 4°C with primary antibodies (rabbit polyclonal anti GFAP 1:700, DakoCytomation, Campbellfield, Australia; mouse polyclonal anti Iba1, 1:200). After 3 rinses in PBS for 10 min each, sections were incubated with an appropriate secondary antibody (1:1,000 ALEXA Fluor 594, 1:200 ALEXA Fluor 488; Molecular Probes, Invitrogen Carlsbad, CA), for 1 h at 37°C. This was followed by three 5-min washes in PBS and counterstaining with DNA-specific label, bisbenzamide (Hoechst) 1:10,000, for 1 min at room temperature (RT) to measure the thickness of the photoreceptor layer (Valter et al. 2005). Images were taken by confocal microscope (Nikon, Tokyo, Japan) and fluorescence microscope (Nikon). The spatial resolution employed was 1,024 × 1,024, the pinhole was set at 1 airy unit (AU) and Z stacks were made with 17 pictures and all stacks were collected using a x40 objective. Final images of all groups were processed in parallel using Adobe Photoshop CS5 software (Adobe Systems Inc., San Jose, CA, USA). Outer nuclear layer (ONL) thickness was measured starting at the dorsal edge along the vertical meridian crossing the optic nerve head according to a procedure already described. Measurements were reported at 1-mm intervals (each point was the mean of four measurements at 250-µm intervals). In each retina, we measured two sections. We measured the pixel intensity of GFAP expression of Müller cells along retinal sections, from the superior to the inferior edge.

Outcome measures

Three criteria of neuroreaction were used, the surviving population of photoreceptors, the rate of microglial activation with Iba1+ cells counting and the expression of the stress-inducible protein GFAP in Müller cells (Gallego et al. 2012; Noailles et al. 2014).

Statistical analysis

The significance of differences in ONL thickness, Iba1+ cells counting and GFAP labeling associated with conditioning were assessed using ANOVA, followed by the multiple comparison Tukey's test. Results are expressed as the mean ± SEM; $p < 0.05$ was considered significant.

RESULTS

Morphological analysis: photoreceptor survival

Fig. 1A shows a representative reconstruction of vertical section of implanted retina with a bisbenzimide labeling. The correct position of the silk implant was maintained with a good preservation of the ONL.

The result is shown quantitatively in Fig. 1B which illustrates ONL thickness in healthy control, implanted eye and internal control as a function of distance between the inferior and superior edges of the retina. ONL thinning induced by silk is relevant only at the retina-silk interface in the superior retina (1st point superior retina: One way ANOVA,* p<0.05; Tukey's test, implanted eye *vs* internal control p=0.739; implanted eye *vs* healthy retina p<0.05; internal control *vs* healthy retina p=0.092—2nd point superior retina: One way ANOVA, *p<0.05; Tukey's test, implanted eye *vs* internal control p<0.05; implanted eye *vs* healthy retina p<0.05; internal control *vs* healthy retina p=0.162— 3rd point superior retina: One way ANOVA, ***p<0.0001; Tukey's test, implanted eye *vs* internal control p<0.001; implanted eye *vs* healthy retina p<0.0001; internal control *vs* healthy retina p=0.428 — 4th point superior retina: One way ANOVA,*** p<0.001; Tukey's test, implanted eye *vs* internal control p<0.05; implanted eye *vs* healthy retina p<0.001; internal control *vs* healthy retina p=0.063).

Fig. 1C shows mean ONL thickness averaged

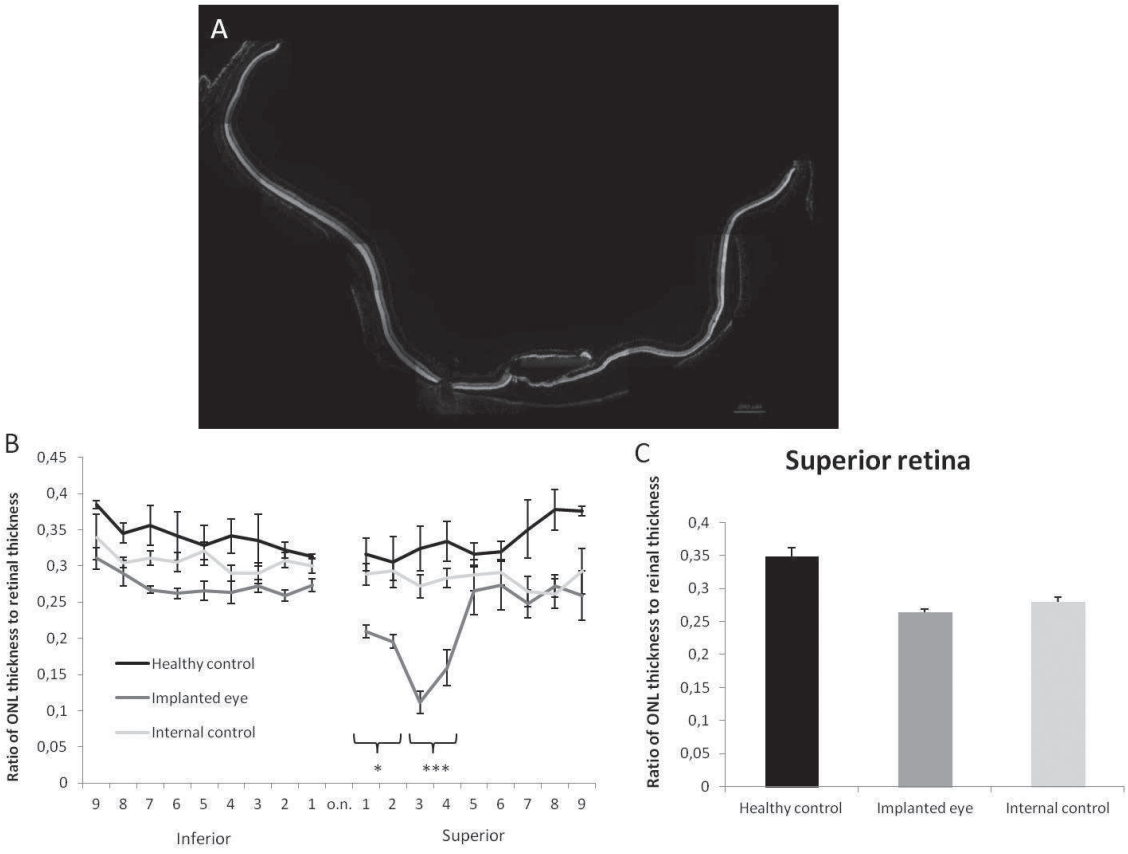

Fig. 1. *Impact of the silk presence on the thickness of the ONL superior retina.* ***A)*** *Reconstruction of vertical section of implanted retina with bisbenzimide labeling. Note the position of the silk under the retina 2 months after surgical insertion of silk.* ***B)*** *Ratio of ONL thickness to retinal thickness, from the superior to the inferior edge through the optic disc (O.D.).* ***C)*** *Ratio of ONL thickness to retinal thickness, in the non-implanted superior area (the superior retinal area without a silk-retina interface). No significant differences among the three groups, p=0.460.*

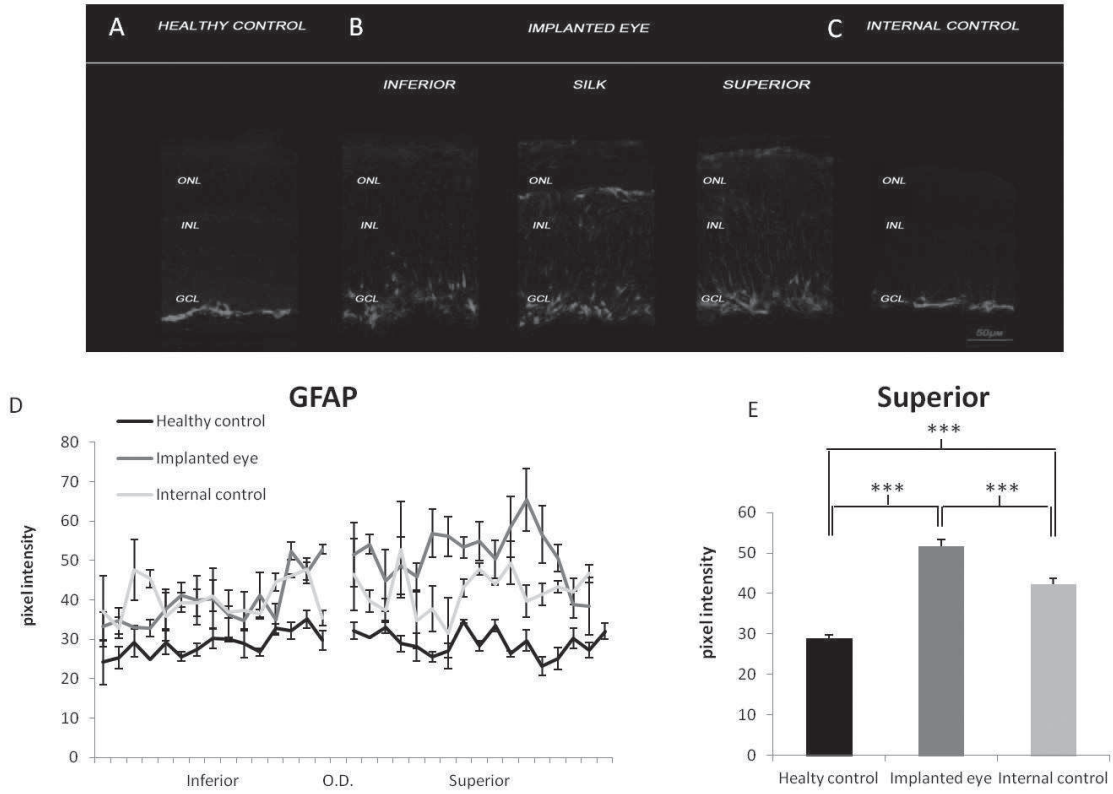

Fig. 2. *Impact of silk presence on GFAP labeling of Müller cells A–C. Representative GFAP labeling in healthy control (**A**), implanted eye (**B**), internal control (**C**) 2 months after surgical insertion of silk. Surgery and silk presence induced the up-regulation of GFAP in the radially oriented Müller cells; the protein is visible along the full length of the Müller cells, from the ILM to the OLM. **D**) Quantification of GFAP expression as a function of distance from superior edge through the optic disc (O.D.). **E**) Mean GFAP expression in the non-implanted superior area (the superior retinal area without a silk-retina interface). The difference among the groups is statistically significant.(One way ANOVA, ***p < 0.001; Tukey's test, implanted eye vs internal control ***p<0.001 implanted eye vs healthy retina ***p<0.001 internal control vs healthy retina ***p<0.001).*

across superior retina, in all experimental groups. The comparison was made by measuring ONL thickness in retinal fields without a silk-retina interface. The difference among the groups is not statistically significant (p=0.460).

Inflammatory marker: impact on GFAP expression

Fig. 2 shows representative images of GFAP expression in the superior retina, in the various experimental groups. In controls, GFAP expression is confined to the astrocytes at the inner surface of the retina (Fig. 2A). Surgical operation and the presence of the silk implant induce a significant up-regulation of GFAP in the radially oriented Müller cells compared to the internal control (Fig. 2C); the protein was visible in Müller cells at the level of the silk implant and in the inferior and superior sides (Fig. 2B).

The result is shown quantitatively in Fig. 2 D, E. The Müller cell labeling was consistent along the superior retina. The difference in the GFAP expression was significant between internal control and implanted group (***p<0.001; Fig. 3E).

Immune response: microglia activation

Fig. 3 shows representative images of activated microglia (Iba1 staining) in the superior retina, in all experimental groups. In control, microglia is located

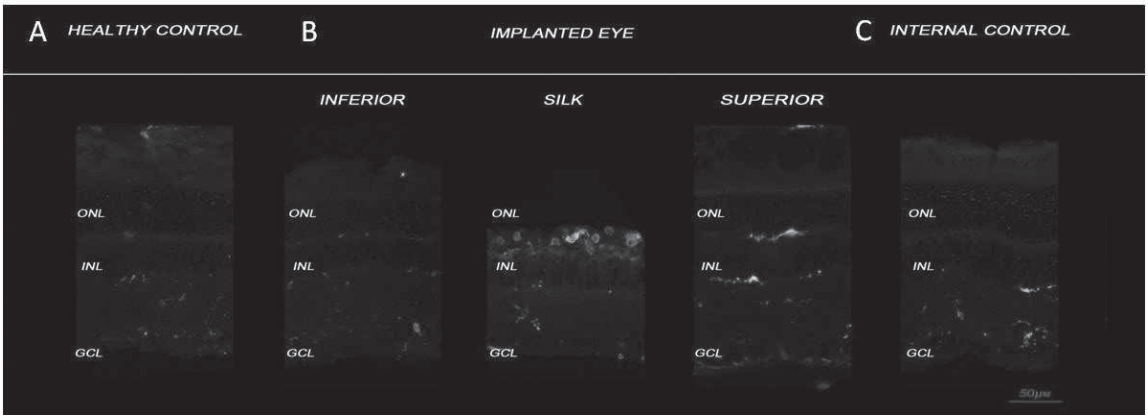

Fig. 3. *Distribution and morphology of microglia activated in (**A**) healthy control, (**B**) implanted eye and (**C**) internal control. Vertical section of the central retina immunolabeled with Iba1. Note presence maximum of Iba1+ cells in correspondence of the silk implant 2 months after implantation.*

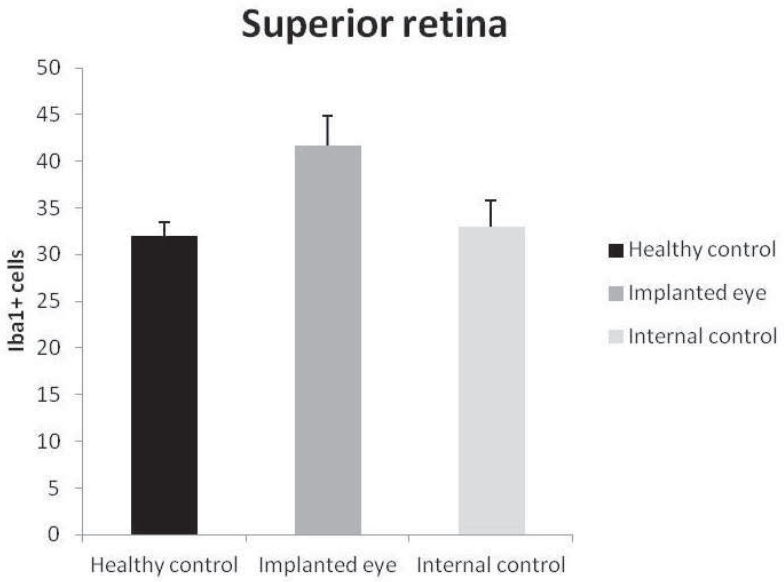

Fig. 4. *Quantification of microglia activated in the healthy control, implanted eye and internal control. Counts of Iba1+ cells in all retinal layers in the portion central superior of the non-implanted superior area (the central superior retinal area without a silk-retina interface). The implanted eye group and the internal control group values were not significantly different (One way ANOVA, p > 0.273).*

in the inner retina (Fig. 3A). Surgical operation and the silk implant produced a microglial activation defined by morphological changes and focal migration (Noailles et al. 2014) in the retina at the level of the implant (Fig. 3B).

The result is shown quantitatively in Fig. 4. IBA1+ cells were counted along the superior retina, without considering silk-retina interface, in the various experimental groups. The difference in the amount of labeled microglial cells, between internal

control and implanted group, was not significant (One way ANOVA $p > 0.273$).

DISCUSSION

Our results show that two months after surgical insertion of a silk-based substrate, the morphology of the retina was highly preserved, suggesting a high level of biocompatibility. As consequence of a low rate of neural cell death, the outer nuclear layer remains of normal thickness, except for a small area close to the implanted silk. As expected, a marked increase in GFAP expression was present in the operated eye, suggestive of an inflammatory response that was not, however, so intense as to induce a significant microglia activation. Altogether our data support silk as a good candidate biomaterial to support retinal visual prosthesis implants.

ACKNOWLEDGEMENTS

Supported by Telethon grant GP12033.

REFERENCES

Butterwick A, Huie P, Jones BW, Marc RE, Marmor M, Palanker D. (2009) Effect of shape and coating of a subretinal prosthesis on its integration with the retina. *Exp Eye Res* **88**(1):22–9.

Coleman RH, Chan CC, Ferris FL, III, and Chew EY (2008) Age-related macular degeneration *Lancet* **372**(9652): 1835–1845.

Curcio CA, Medeiros NE, Millican CL (1996) Photoreceptor loss in age-related macular degeneration. *Invest Ophthalmol Vis Sci* **37**: 1236–1249.

Gallego BI, Salazar JJ, Hoz R, Rojas B, Ramírez AI, Salinas-Navarro M, Ortín-Martínez A , Valiente-Soriano FJ , Avilés-Trigueros M , Villegas-Perez MP, Vidal-Sanz M, Triviño A, Ramírez JM (2012) IOP induces upregulation of GFAP and MHC-II and microglia reactivity in mice retina contralateral to experimental glaucoma. *J Neuroinflammation* **9**:92

Light JG, Fransen JW, Adekunle AN, Adkins A, Pangeni G, Loudin J, Mathieson K, Palanker DV, McCall MA, Pardue MT (2014) Inner retinal preservation in rat models of retinal degeneration implanted with subretinal photovoltaic arrays. *Exp Eye Res* **128**:34-42

Liu X, Zhang Y, He Y, Zhao J, Su G (2015) Progress in histopathologic and pathogenesis research in a retinitis pigmentosa model. *Histol Histopathol.* **11**:11596.

Maghami MH, Sodagar AM, Lashay A, Riazi-Esfahani H, Riazi-Esfahani M Visual prostheses: the **enabling technology** to **give sight** to the **blind (2014)** *J Ophthalmic Vis Res* **9(4)**:494-505.

Noailles A, Fernández-Sánchez L, Lax P, Cuenca N (2014) Microglia activation in a model of retinal degeneration and TUDCA neuroprotective effects. *J. Neuroinflammation* **11**: 186.

Valter K, Bisti S, Gargini C, Di Loreto S, Maccarone R, Cervetto L, Stone J (2005) Timecourse of neurotrophic factor upregulation and retinal protection against light damage following optic nerve section. *Invest Ophthalmol Vis Sci* **46**:1748–175.